

# Large family candidates for kagome topological superconductors

Xin-Wei Yi,<sup>1</sup> Xing-Yu Ma,<sup>1</sup> Zhen Zhang,<sup>1</sup> Zheng-Wei Liao,<sup>1</sup> Jing-Yang You,<sup>2,\*</sup> and Gang Su<sup>3,1,†</sup>

<sup>1</sup>*School of Physical Sciences, University of Chinese Academy of Sciences, Beijing 100049, China*

<sup>2</sup>*Department of Physics, Faculty of Science, National University of Singapore, 117551, Singapore*

<sup>3</sup>*Kavli Institute for Theoretical Sciences, and CAS Center for Excellence in Topological Quantum Computation, University of Chinese Academy of Sciences, Beijing 100190, China*

A group of newly discovered non-magnetic metal kagome structures  $AV_3Sb_5$  ( $A=K, Rb, Cs$ ) have aroused widespread interest in experiment and theory due to their unusual charge density wave (CDW) and intertwined superconductivity. However, they all possess weak electron-phonon coupling (EPC) and low superconducting transition temperature. Here, we performed high-throughput first-principles calculations on novel kagome candidates with  $AV_3Sb_5$  prototype structure, and proposed 24 dynamically stable novel kagome metals. The calculation based on Bardeen-Cooper-Schrieffer theory shows that most of these metals are superconductors with much stronger EPC than the reported  $AV_3Sb_5$  materials, and their superconducting transition temperatures  $T_c$  is between 0.3 and 5.0K. Additionally, several compounds, such as  $KZr_3Pb_5$  with the highest  $T_c$ , are identified as  $\mathbb{Z}_2$  topological metals with clear Dirac cone topological surface states near Fermi level.  $NaZr_3As_5$  is shown to have possible CDW phases. Our results provide rich platforms for exploring various new physics with the prototype kagome structure, in which the coexistence of superconductivity and nontrivial topological nature provides promising insights on the discovery of topological superconductors.

*Introduction.*—In 2019, a new class of nonmagnetic metals  $AV_3Sb_5$  ( $A=K, Rb, \text{ and } Cs$ ) with perfect vanadium kagome net were synthesized [1]. Since then, surprises have emerged in the study of these structures. The electronic structures of  $AV_3Sb_5$  show Dirac nodal lines, nontrivial  $\mathbb{Z}_2$  topological indices of bands and clear topological surface near Fermi level, showing that their normal states are  $\mathbb{Z}_2$  topological metals [1–4]. The superconducting transition temperatures  $T_c$  of  $KV_3Sb_5$ ,  $RbV_3Sb_5$  and  $CsV_3Sb_5$  are 0.93 [2], 0.92 [5] and 2.5K [3] (2.3K [6, 7]), respectively, in which the corresponding transition temperatures  $T^*$  of charge density wave (CDW) order are 78 [8], 102 [9] and 94K [10], respectively. The exotic CDW states without electron-phonon coupling (EPC) mechanism [9] display many unconventional characteristics. The CDWs in these three compounds exhibit chiral anisotropy [11–13] and reduce the density of electronic states near the Fermi level [11, 14–16]. Various evidence including giant anomalous Hall response even without magnetic field [17, 18], the chirality of CDW that can be tuned by a magnetic field [11–13], edge supercurrent [19] and spontaneous internal magnetic field [20] indicates that the charge order may break the time-reversal symmetry, which has also been verified theoretically [11, 21, 22]. Moreover, it has been found that  $CsV_3Sb_5$  samples have the roton pair density wave [7], which is analogous to the one in unconventional high- $T_c$  cuprate superconductors [23]. The coexistence of V- and U-shaped superconducting gaps in  $CsV_3Sb_5$  [24] and the anisotropic superconducting properties [25] imply a possible multi-band superconducting pairing. Intertwined superconductivity with CDW shows many new features. For instance,  $T_c$  exhibits an unconventional double dome behavior, and  $T^*$  decreases rapidly with increasing pressure [10, 26, 27]. The second dome of  $T_c$

and the disappearance of  $T^*$  emerge at the same pressure. The superconducting properties and charge order of  $AV_3Sb_5$  can also be tuned by magnetic impurities [24], strain [28], thicknesses [29–31], which dramatically enrich the phase diagram. The experimental and theoretical studies on  $AV_3Sb_5$  show a complementary and rapid trend. However, to further explore the exotic properties of  $AV_3Sb_5$ , more candidate compounds based on  $AV_3Sb_5$  prototype structure appear to be needed.

In this paper, we first apply the high-throughput first-principles calculations on 800 new kagome structures based on  $AV_3Sb_5$  prototype. We found 24 dynamic stable new metal compounds. Then, we calculated their superconducting and topological properties. The results show that 14 novel compounds are superconductors with superconducting transition temperatures between 0.3 and 5.0K. Some compounds, including  $KZr_3Pb_5$  with the highest superconducting transition temperature, have strong  $\mathbb{Z}_2$  indices with abundant nontrivial topological surface states near Fermi surface, showing they are  $\mathbb{Z}_2$  topological metals. The coexistence of superconductivity and nontrivial topology in  $KZr_3Pb_5$  and some other compounds opens a door for the possible discovery of topological superconductor based on the kagome net. Additionally, we also found two possible CDW phases in  $NaZr_3As_5$ , which exhibit soft modes in phonon spectrum, and may provide useful information for further understanding the CDW phases in  $AV_3Sb_5$ .

*Crystal structures of  $AV_3Sb_5$ .*—The  $AV_3Sb_5$  crystal- lize in the hexagonal structure with the space group of  $P6/mmm$  (No.191) as shown in Fig. 1. As we can see, these three-dimensional (3D) compounds form a layered structure. The perfect kagome net of V atoms mixed with a simple triangular net of Sb atoms is located in the middle layer, which is sandwiched by two additional

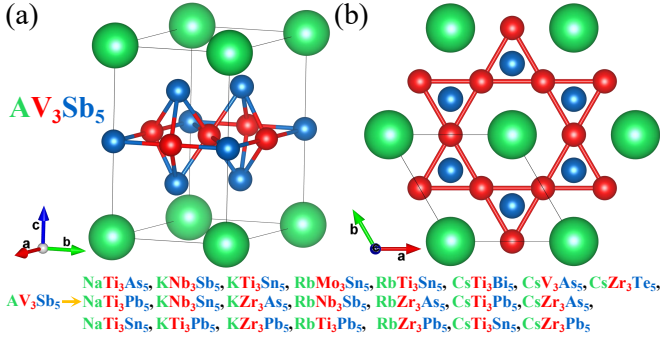


FIG. 1. The crystal structure of  $AV_3Sb_5$ . 22 new stable  $AB_3C_5$  members with the same crystal structure as  $AV_3Sb_5$  are also indicates.

honeycomb layers of Sb atoms. The upper and lower triangular layers of alkali metal A atoms have large bond distances with respect to the middle V-Sb layer and are loosely bonded to them.

*Searching new structures.*—The high-throughput first-principles calculations are used to search for kagome topological superconductor candidates (as indicated in Fig. S1 in Supplementary Material (SM)). Based on the prototype structure of  $AV_3Sb_5$ , 800 new compounds are constructed by replacing A with alkali metal elements Li, Na, K, Rb and Cs, replacing V with all transition metal elements in the fourth and fifth periods of the periodic table, and replacing Sb with its neighboring elements (Ge, As, Se, Sn, Sb, Te, Pb, and Bi). These new compounds will be abbreviated as  $AB_3C_5$  below. For all these new compounds, we first carry out fully geometric relaxation in different magnetic configurations (shown Fig. S2). Then, by comparing the total energies of different magnetic configurations, each  $AB_3C_5$  member can be classified according to nonmagnetic (NM), ferromagnetic (FM) and antiferromagnetic (AFM) configurations. The phonon spectrum is calculated to determine the dynamic stability of these  $AB_3C_5$  members. Compounds without imaginary frequency in phonon spectra will be further analyzed for corresponding electronic structures, superconductivity, and topological properties. On the other hand, the phonon spectra with imaginary frequency will be used to discuss possible CDW phases.

In doing so, we discovered 24 stable novel  $AB_3C_5$  members, including 22 non-magnetic structures, one FM  $CsTi_3Pb_5$  with a magnetic moment of  $0.69 \mu_B$  per Ti atom and one AFM  $RbCr_3Te_5$  with a magnetic moment of  $2.33 \mu_B$  per Cr atom. Their lattice information is listed in Table S1. The electronic structures show that they are all metals similar to  $AV_3Sb_5$ . Furthermore, 22 members keep the same crystal structure as  $AV_3Sb_5$  after structural optimization (as listed in Fig. 1), except for  $CsRu_3Ge_5$  and  $RbCr_3Te_5$ , whose triangles in the kagome nets are twisted, which changes their space group to  $P\bar{6}2m$ .

TABLE I. Electronic density of states at Fermi energy  $N(E_F)$  for per fomular unit ( $eV^{-1}f.u.^{-1}$ ), logarithmic average frequency  $\omega_{log}$  (K), EPC  $\lambda(\omega = \infty)$  and  $T_c$  of 14 stable compounds.

	$N(E_F)$ ( $eV^{-1}f.u.^{-1}$ )	$\omega_{log}$ (K)	$\lambda$	$T_c$ (K)
RbMo <sub>3</sub> Sn <sub>5</sub>	3.60	136.5	0.36	0.371
KNb <sub>3</sub> Sn <sub>5</sub>	4.22	149.1	0.52	2.102
CsRu <sub>3</sub> Ge <sub>5</sub>	3.19	170.8	0.36	0.353
CsTi <sub>3</sub> Bi <sub>5</sub>	5.96	163.4	0.35	0.316
KTi <sub>3</sub> Pb <sub>5</sub>	7.29	157.9	0.51	2.039
RbTi <sub>3</sub> Pb <sub>5</sub>	7.50	156.5	0.50	1.857
KTi <sub>3</sub> Sn <sub>5</sub>	6.57	180.3	0.42	0.974
RbTi <sub>3</sub> Sn <sub>5</sub>	6.50	182.5	0.42	0.961
CsTi <sub>3</sub> Sn <sub>5</sub>	6.87	174.6	0.45	1.375
CsZr <sub>3</sub> As <sub>5</sub>	3.40	125.8	0.56	2.289
KZr <sub>3</sub> Pb <sub>5</sub>	6.47	94.1	0.91	5.027
RbZr <sub>3</sub> Pb <sub>5</sub>	6.56	111.9	0.72	4.154
CsZr <sub>3</sub> Pb <sub>5</sub>	6.53	119.2	0.58	2.438
CsZr <sub>3</sub> Te <sub>5</sub>	2.88	123.5	0.48	1.266

*Superconductivity.*—The metallicity of these 24  $AB_3C_5$  members enables us to perform further calculations on superconductivity. We calculated the Eliashberg electron-phonon spectral function  $\alpha^2F(\omega)$  and cumulative frequency dependent EPC  $\lambda(\omega)$  of these materials at ambient pressure, and then the superconducting transition temperature  $T_c$  can be estimated with the McMillan-Allen-Dynes approach of Bardeen-Cooper-Schrieffer (BCS) theory (See SM for detailed calculations). After careful calculation and screening, we found that 14 of these 24 members have superconducting ground states as listed in Table I, where  $KZr_3Pb_5$  possesses the highest  $T_c$  of 5.027K, which is more than twice the experimental values of  $AV_3Sb_5$  (see Table II) [2, 3, 5–7].

We choose  $AZr_3Pb_5$  group with relative higher superconducting transition temperatures for further discussions. The phonon spectra, phonon density of states

TABLE II. Electronic density of states at Fermi energy  $N(E_F)$  ( $eV^{-1}f.u.^{-1}$ ), EPC  $\lambda(\omega = \infty)$ , calculated  $T_c$  and experimental superconducting temperature  $T_c^{exp}$  for the ISD phase of  $AV_3Sb_5$  [2, 3, 5–7, 32] and pristine phase of  $AZr_3Pb_5$ .

	$N(E_F)$ ( $eV^{-1}f.u.^{-1}$ )	$\lambda$	$T_c$ (K)	$T_c^{exp}$ (K)
KV <sub>3</sub> Sb <sub>5</sub>	2.9	0.38	0.22	0.93
RbV <sub>3</sub> Sb <sub>5</sub>	2.33	0.32	0.05	0.92
CsV <sub>3</sub> Sb <sub>5</sub>	1.30	0.25	0.0008	2.5 (2.3)
KZr <sub>3</sub> Pb <sub>5</sub>	6.47	0.91	5.027	?
RbZr <sub>3</sub> Pb <sub>5</sub>	6.56	0.72	4.154	?
CsZr <sub>3</sub> Pb <sub>5</sub>	6.53	0.58	2.438	?

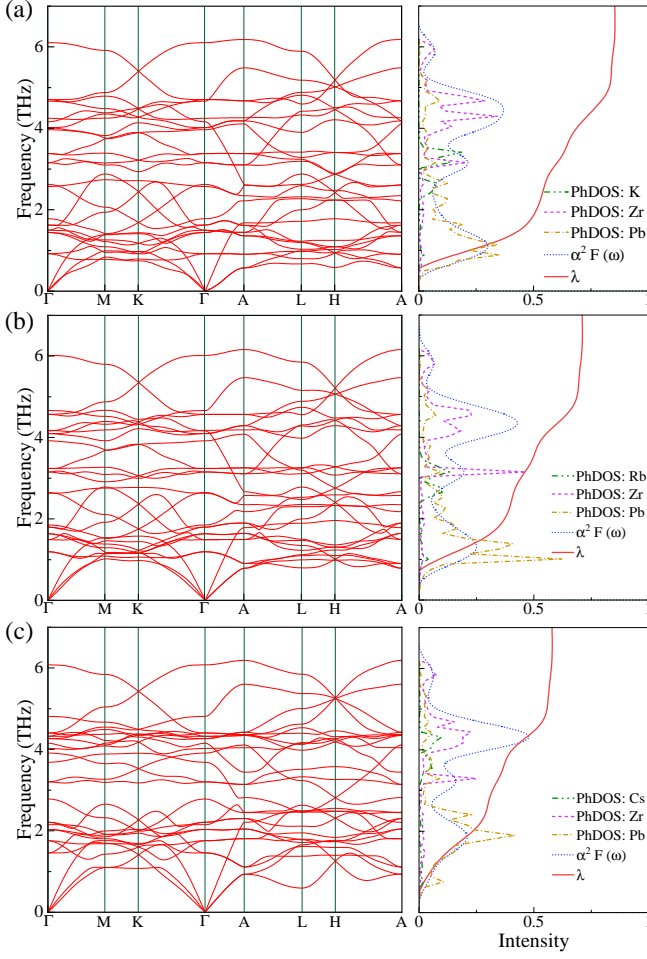


FIG. 2. The phonon spectra, projected PhDOS, Eliashberg spectral function  $\alpha^2F(\omega)$ , and cumulative frequency dependent EPC  $\lambda(\omega)$  of (a)  $KZr_3Pb_5$ , (b)  $RbZr_3Pb_5$ , (c)  $CsZr_3Pb_5$ .

(PhDOS),  $\alpha^2F(\omega)$  and  $\lambda(\omega)$  of the three structures are plotted in Fig. 2. We can see that the phonon spectra of three compounds are very similar. Careful comparison of their phonon spectra shows that the faint phonon softening at L point gradually becomes obvious from K to Rb to Cs. It can be seen from PhDOS that the contributions of Pb and Zr atoms to PhDOS is mainly distributed in the relatively low and high frequency regions with much high peaks, respectively, while the PhDOS of alkali metal atoms distributed in the medium frequency region are very small. The relatively low frequency ( $<3$ THz) phonons corresponding to the vibration modes of Pb account for more than half of the total EPC. The  $T_c$  of the three compounds decreases with the gradual increase of the atomic number of alkali metals as shown in Table I. The gradual decrease of  $T_c$  from K to Rb to Cs is due to the negligible contribution of alkali metal elements to the EPC, and the increase of atomic radius from K to Cs, resulting in the gradual increase of the lattice parameters, is equivalent to applying a negative pressure

(tensile strain) to the lattice, which significantly reduce the parameters related to the lattice and weakens the EPC.

*Electronic band structure and topological property.*— We plot the calculated electronic energy bands and density of states (DOS) with spin-orbit coupling (SOC) for  $KZr_3Pb_5$  in Fig. 3(a). The electronic band structures of  $RbZr_3Pb_5$  and  $CsZr_3Pb_5$  are given in Figs. S21-22. The 3D Fermi surface (FS) of  $KZr_3Pb_5$  and its 2D map at  $k_z=0$  and  $k_z=\pi$  slices are drawn in Figs. 3(b)-(d), which is obviously different from the FS of  $AV_3Sb_5$  that exhibits a strong 2D feature. Furthermore, we can see the obvious Fermi surface nesting with the nesting vector parallel to A-L and A-H in the  $k_z=\pi$  slice.

Unlike most magnetic kagome metal materials,  $AZr_3Pb_5$  is nonmagnetic similar to  $AV_3Sb_5$ . So combining both time-reversal symmetry and inversion symmetries of  $AZr_3Pb_5$ , we can get their  $\mathbb{Z}_2$  topological invariants by calculating the parity of the wave functions at all time-reversal invariant momenta (TRIM) points [33]. It can be seen from Fig. 3(e) that several energy bands passing through the Fermi surface all have strong topological  $\mathbb{Z}_2$  indices, resulting in abundant Dirac cone surface states at TRIM M-point near the Fermi level as shown in Figs. 3 (g) and (h). The continuous bandgap between two energy bands in the whole Brillouin zone, the nontrivial topological surface states and the strong  $\mathbb{Z}_2$  indices of bands near the Fermi level make  $KZr_3Pb_5$  a  $\mathbb{Z}_2$  topological metal. Similar analysis shows that many other  $AB_3C_5$  members, such as  $CsZr_3Pb_5$ , are also  $\mathbb{Z}_2$

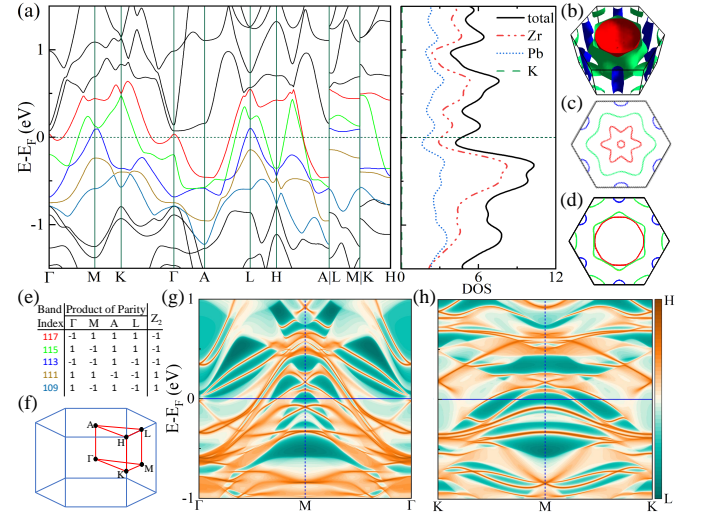


FIG. 3. (a) The electronic energy bands and density of states calculated with SOC for  $KZr_3Pb_5$ . (b) 3D FS of  $KZr_3Pb_5$ , and its 2D maps at (c)  $k_z=0$  and (d)  $\pi$  slices. Different colors of FS refers to different band indices consistent with (a). (e) Product of parity and  $\mathbb{Z}_2$  indices of bands near Fermi level. (f) The Brillouin zone with high symmetry paths indicated. Topological surface states along (g)  $\Gamma$ -M- $\Gamma$  and (h) K-M-K paths on (001) plane for  $KZr_3Pb_5$ .

topological metals.

*Possible CDW phases.*—We take  $\text{NaZr}_3\text{As}_5$  for an example to explore possible CDW phases. One may find that the phonon spectrum in Fig. 4(d) shows clear softening acoustic phonon modes near M and L points at the Brillouin zone boundary, and the imaginary frequency at L point is slightly larger than that at M point, which is very similar to  $\text{AV}_3\text{Sb}_5$  [15, 32]. The symmetry analysis on  $\text{AV}_3\text{Sb}_5$  indicates that the irreducible representations of the imaginary modes at M and L points are  $M_1^+$  and  $L_2^-$ , respectively, which is also consistent with the previous studies [15, 34]. However, similar analysis shows the irreducible representations of imaginary modes in  $\text{NaZr}_3\text{As}_5$  are  $M_2^+$  and  $L_1^-$ , which makes  $\text{NaZr}_3\text{As}_5$  exhibit completely different distortions from  $\text{AV}_3\text{Sb}_5$ . In consideration of one M and one L points, it gives the phase as seen in Fig. 4(b). The soft mode at M point makes corner-sharing triangles in layers rotate around the corner, while the soft mode at L point makes the distortion of adjacent layers have a  $\pi$ -shift. Clockwise and counterclockwise distortions generate the same structure. The combination of all three unequal M and L points gives a similar phase as shown in Fig. 4(c), which differs from Fig. 4(b) in that Zr atoms in the kagome layers rotate around the center of triangles. These two structures have Ibam (No.72) and P6/mcc (No.192) space groups, respectively. Both of them reduce the  $C_6$  rotation symmetry to  $C_2$ , but still retain the space inversion symmetry.

Their phonon spectra in Figs. 4(e) and (f) are dynamically stable with completely disappeared imaginary fre-

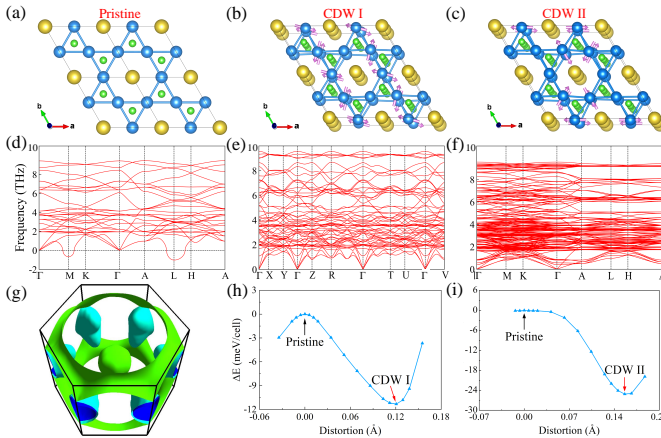


FIG. 4. Crystal structures of  $\text{NaZr}_3\text{As}_5$  in the (a)  $2 \times 2$  supercell of pristine phase, (b) CDW I phase, and (c) the CDW II phase and their corresponding phonon spectra (d), (e) and (f), respectively. (g) 3D FS of  $\text{NaZr}_3\text{As}_5$ . The comparison of total energies  $\Delta E$  for (h) pristine phase and CDW I, (i) pristine phase and CDW II, where the distortion represents the displacement of Zr atoms and  $\Delta E$  stands for the relative total energy with respect to the pristine phase per with 72 atoms.

quency, so both of them have possible CDW phases of  $\text{NaZr}_3\text{As}_5$ . We label them CDW I and CDW II, respectively. Compared with the pristine phase, the displacement values of Zr atoms in kagome layers in CDW I and CDW II are 0.12 and 0.15 Å, respectively. The total energy as a function of displacement of Zr atoms is shown in Figs. 4(h) and (i). The total energies of the two stable CDW phases are 11.3 and 25.1 meV lower than the pristine structure, respectively.

The real CDW phase and the possible competition or cooperation between charge order and superconductivity in  $\text{NaZr}_3\text{As}_5$  deserve the experimental exploration. Besides  $\text{NaZr}_3\text{As}_5$ , we also list those structures with obvious soft modes at high symmetry paths that may have CDW phases as well in Fig. S27.

*Discussion.*—In addition to  $\text{AZr}_3\text{Pb}_5$ , the band structures with or without SOC, DOS, FS, phonon spectra of all other dynamically stable  $\text{AB}_3\text{C}_5$  members are presented in Figs. S3-23 in SM. The new  $\text{AV}_3\text{C}_5$  members are not only structurally similar to  $\text{AV}_3\text{Sb}_5$ , but also inherit many attractive features, such as the existence of Van Hove singularities at high symmetry points near the Fermi level, Dirac points at the Fermi level, Dirac nodal lines, and strong 2D properties of the phonon spectrum and FS, which deserve further studies.

An important feature of those predicted structures beyond  $\text{AV}_3\text{Sb}_5$  is their much stronger EPC strengths. The calculated  $T_c$  of  $\text{KV}_3\text{Sb}_5$ ,  $\text{RbV}_3\text{Sb}_5$ , and  $\text{CsV}_3\text{Sb}_5$  based on BCS theory are 0.0008, 0.05 and 0.22 K, respectively [32], which are much lower than their experimental values (see Table II), because the CDW in  $\text{AV}_3\text{Sb}_5$  reduces the DOS near Fermi level and suppresses BCS superconductivity. This indicates there may be an unconventional superconducting mechanism. This mechanism is also expected to appear in materials listed in Table I. From Table II, it can be observed that the calculated  $T_c$  of  $\text{AZr}_3\text{Pb}_5$  are much higher than those of  $\text{AV}_3\text{Sb}_5$ , and thereby experimental  $T_c$  of  $\text{AZr}_3\text{Pb}_5$  may be further considerably high.

The coexistence of superconductivity and topological nontrivial surface states is essentially rare [35–38]. It was reported that the robust zero-bias conductance peak in  $\text{CsV}_3\text{Sb}_5$  exhibits similar characteristics to the  $\text{Bi}_2\text{Te}_3/\text{NbSe}_2$  heterostructures with Majorana bound state [6]. Our new compounds with both the superconducting ground state and the nontrivial topological surface states near the Fermi surface would provide a rich platform for exploring topological superconductivity and Majorana zero-energy modes.

Mature experimental methods like flux method have been used to synthesize high-quality and stable  $\text{AV}_3\text{Sb}_5$  compounds, which is a prerequisite for the rapid development of experimental analysis. In the initial work of Brenden *et al.* for the  $\text{AV}_3\text{Sb}_5$  family, they explored the combination of (K, Rb, Cs)(V, Nb, Ta)(Sb, Bi) under different synthetic conditions [1]. However, only  $\text{KV}_3\text{Sb}_5$ ,

RbV<sub>3</sub>Sb<sub>5</sub>, and CsV<sub>3</sub>Sb<sub>5</sub> were crystallized. In this work, 800 AB<sub>3</sub>C<sub>5</sub> members in the high-throughput screening process contain most of the combinations they explored. Our calculation results show that those compounds not synthesized in their experiment are dynamically unstable except KNb<sub>3</sub>Sb<sub>5</sub>. The agreement with the experimental results indicates that our present calculations are reasonable, and the stable structures presented here are likely to be synthesized in future experiments. Very recently, a newly discovered family of kagome metals RV<sub>6</sub>Sn<sub>6</sub> (R = Gd, Ho, Y) with two V-derived kagome layers in the primitive cell was also synthesized by flux method [39, 40]. Therefore, the versatile and matured flux method could be employed to synthesize the stable structures in Table S1.

*Summary.*—In conclusion, we calculated 800 new kagome candidates based on the prototype structure of AV<sub>3</sub>Sb<sub>5</sub> using a high-throughput DFT screening process, and discovered 24 dynamically stable novel metal compounds, including one ferromagnetic, one antiferromagnetic and 22 nonmagnetic structures. These compounds display many appealing properties similar to AV<sub>3</sub>Sb<sub>5</sub>. Furthermore, based on the McMillan-Allen Dynes approach, 14 compounds among them were predicted to be phonon-mediated BCS superconductors with the superconducting transition temperature  $T_c$  between 0.3-5K. KZr<sub>3</sub>Pb<sub>5</sub> with the highest  $T_c$  exhibits strong  $\mathbb{Z}_2$  invariants of the energy bands and abundant nontrivial topological surface states near the Fermi level, revealing that it is a  $\mathbb{Z}_2$  topological metal. In addition, we also found two possible CDW phases in NaZr<sub>3</sub>As<sub>5</sub>. This present work would give more insights on the exploration of possible topological superconductors.

## ACKNOWLEDGMENTS

This work is supported in part by the National Key R&D Program of China (Grant No. 2018YFA0305800), the Strategic Priority Research Program of the Chinese Academy of Sciences (Grants No. XDB28000000), the National Natural Science Foundation of China (Grant No.11834014), and High-magnetic field center of Chinese Academy of Sciences.

\* phyjyy@nus.edu.sg

† gsu@ucas.ac.cn

- [1] B. R. Ortiz, L. C. Gomes, J. R. Morey, M. Winiarski, M. Bordelon, J. S. Mangum, I. W. H. Oswald, J. A. Rodriguez-Rivera, J. R. Neilson, S. D. Wilson, E. Ertekin, T. M. McQueen, and E. S. Toberer, New kagome prototype materials: discovery of KV<sub>3</sub>Sb<sub>5</sub>, RbV<sub>3</sub>Sb<sub>5</sub>, and CsV<sub>3</sub>Sb<sub>5</sub>, *Phys. Rev. Materials* **3**, 094407 (2019).
- [2] B. R. Ortiz, P. M. Sarte, E. M. Kenney, M. J. Graf, S. M. L. Teicher, R. Seshadri, and S. D. Wilson, Superconductivity in the z2 kagome metal KV<sub>3</sub>Sb<sub>5</sub>, *Phys. Rev. Materials* **5**, 034801 (2021).
- [3] B. R. Ortiz, S. M. Teicher, Y. Hu, J. L. Zuo, P. M. Sarte, E. C. Schueller, A. M. Abeykoon, M. J. Krogstad, S. Rosenkranz, R. Osborn, R. Seshadri, L. Balents, J. He, and S. D. Wilson, CsV<sub>3</sub>Sb<sub>5</sub> : A z2 topological kagome metal with a superconducting ground state, *Phys. Rev. Lett.* **125**, 247002 (2020).
- [4] J. Zhao, W. Wu, Y. Wang, and S. A. Yang, Electronic correlations in the normal state of the kagome superconductor KV<sub>3</sub>Sb<sub>5</sub>, *Phys. Rev. B* **103**, 124117 (2021).
- [5] Q. Yin, Z. Tu, C. Gong, Y. Fu, S. Yan, and H. Lei, Superconductivity and normal-state properties of kagome metal RbV<sub>3</sub>Sb<sub>5</sub> single crystals, *Chinese Phys. Lett.* **38**, 037403 (2021).
- [6] Z. Liang, X. Hou, F. Zhang, W. Ma, P. Wu, Z. Zhang, F. Yu, J.-J. Ying, K. Jiang, L. Shan, Z. Wang, and X.-H. Chen, Three-dimensional charge density wave and surface-dependent vortex-core states in a kagome superconductor CsV<sub>3</sub>Sb<sub>5</sub>, *Phys. Rev. X* **11**, 031026 (2021).
- [7] H. Chen, H. Yang, B. Hu, Z. Zhao, J. Yuan, Y. Xing, G. Qian, Z. Huang, G. Li, Y. Ye, S. Ma, S. Ni, H. Zhang, Q. Yin, C. Gong, Z. Tu, H. Lei, H. Tan, S. Zhou, C. Shen, X. Dong, B. Yan, Z. Wang, and H.-J. Gao, Roton pair density wave in a strong-coupling kagome superconductor, *Nature* **599**, 222 (2021).
- [8] Z. Zhang, Z. Chen, Y. Zhou, Y. Yuan, S. Wang, J. Wang, H. Yang, C. An, L. Zhang, X. Zhu, Y. Zhou, X. Chen, J. Zhou, and Z. Yang, Pressure-induced reemergence of superconductivity in the topological kagome metal CsV<sub>3</sub>Sb<sub>5</sub>, *Phys. Rev. B* **103**, 224513 (2021).
- [9] H. Li, T. Zhang, T. Yilmaz, Y. Pai, C. Marvinnay, A. Said, Q. Yin, C. Gong, Z. Tu, E. Vescovo, C. Nelson, R. Moore, S. Murakami, H. Lei, H. Lee, B. Lawrie, and H. Miao, Observation of unconventional charge density wave without acoustic phonon anomaly in kagome superconductors AV<sub>3</sub>Sb<sub>5</sub> (a=rb, cs), *Phys. Rev. X* **11**, 031050 (2021).
- [10] K. Chen, N. Wang, Q. Yin, Y. Gu, K. Jiang, Z. Tu, C. Gong, Y. Uwatoko, J. Sun, H. Lei, J. Hu, and J.-G. Cheng, Double superconducting dome and triple enhancement of  $t_c$  in the kagome superconductor CsV<sub>3</sub>Sb<sub>5</sub> under high pressure, *Phys. Rev. Lett.* **126**, 247001 (2021).
- [11] Y.-X. Jiang, J.-X. Yin, M. M. Denner, N. Shumiya, B. R. Ortiz, G. Xu, Z. Guguchia, J. He, M. S. Hossain, X. Liu, J. Ruff, L. Kautzsch, S. S. Zhang, G. Chang, I. Belopolski, Q. Zhang, T. A. Cochran, D. Multer, M. Litskevich, Z.-J. Cheng, X. P. Yang, Z. Wang, R. Thomale, T. Neupert, S. D. Wilson, and M. Z. Hasan, Unconventional chiral charge order in kagome superconductor KV<sub>3</sub>Sb<sub>5</sub>, *Nat. Mater.* **20**, 1353 (2021).
- [12] Z. Wang, Y.-X. Jiang, J.-X. Yin, Y. Li, G.-Y. Wang, H.-L. Huang, S. Shao, J. Liu, P. Zhu, N. Shumiya, M. S. Hossain, H. Liu, Y. Shi, J. Duan, X. Li, G. Chang, P. Dai, Z. Ye, G. Xu, Y. Wang, H. Zheng, J. Jia, M. Z. Hasan, and Y. Yao, Electronic nature of chiral charge order in the kagome superconductor CsV<sub>3</sub>Sb<sub>5</sub>, *Phys. Rev. B* **104**, 075148 (2021).
- [13] N. Shumiya, M. S. Hossain, J.-X. Yin, Y.-X. Jiang, B. R. Ortiz, H. Liu, Y. Shi, Q. Yin, H. Lei, S. S. Zhang, G. Chang, Q. Zhang, T. A. Cochran, D. Multer, M. Litskevich, Z.-J. Cheng, X. P. Yang, Z. Guguchia,

- S. D. Wilson, and M. Z. Hasan, Intrinsic nature of chiral charge order in the kagome superconductor RbV3sb5, *Phys. Rev. B* **104**, 035131 (2021).
- [14] E. Uykur, B. R. Ortiz, S. D. Wilson, M. Dressel, and A. A. Tsirlin, Optical detection of charge-density-wave instability in the non-magnetic kagome metal kv3sb5, (2021), [arXiv:2103.07912 \[cond-mat.str-el\]](#).
- [15] N. Ratcliff, L. Hallett, B. R. Ortiz, S. D. Wilson, and J. W. Harter, Coherent phonon spectroscopy and inter-layer modulation of charge density wave order in the kagome metal CsV3sb5, *Phys. Rev. Materials* **5**, 1111801 (2021).
- [16] S. Cho, H. Ma, W. Xia, Y. Yang, Z. Liu, Z. Huang, Z. Jiang, X. Lu, J. Liu, Z. Liu, J. Li, J. Wang, Y. Liu, J. Jia, Y. Guo, J. Liu, and D. Shen, Emergence of new van hove singularities in the charge density wave state of a topological kagome metal RbV3sb5, *Phys. Rev. Lett.* **127**, 236401 (2021).
- [17] F. H. Yu, T. Wu, Z. Y. Wang, B. Lei, W. Z. Zhuo, J. J. Ying, and X. H. Chen, Concurrence of anomalous hall effect and charge density wave in a superconducting topological kagome metal, *Phys. Rev. B* **104**, 1041103 (2021).
- [18] S.-Y. Yang, Y. Wang, B. R. Ortiz, D. Liu, J. Gayles, E. Derunova, R. Gonzalez-Hernandez, L. Šmejkal, Y. Chen, S. S. P. Parkin, S. D. Wilson, E. S. Toberer, T. McQueen, and M. N. Ali, Giant, unconventional anomalous hall effect in the metallic frustrated magnet candidate, KV 3 sb 5, *Sci. Adv.* **6**, 6003 (2020).
- [19] Y. Wang, S. Yang, P. K. Sivakumar, B. R. Ortiz, S. M. L. Teicher, H. Wu, A. K. Srivastava, C. Garg, D. Liu, S. S. P. Parkin, E. S. Toberer, T. McQueen, S. D. Wilson, and M. N. Ali, Proximity-induced spin-triplet superconductivity and edge supercurrent in the topological kagome metal,  $K_{1-x}V_3Sb_5$ , (2020), [arXiv:2012.05898 \[cond-mat.supr-con\]](#).
- [20] C. M. III, D. Das, J. X. Yin, H. Liu, R. Gupta, Y. X. Jiang, M. Medarde, X. Wu, H. C. Lei, J. J. Chang, P. Dai, Q. Si, H. Miao, R. Thomale, T. Neupert, Y. Shi, R. Khasanov, M. Z. Hasan, H. Luetkens, and Z. Guguchia, Time-reversal symmetry-breaking charge order in a kagome superconductor, (2021), [arXiv:2106.13443 \[cond-mat.mtrl-sci\]](#).
- [21] M. M. Denner, R. Thomale, and T. Neupert, Analysis of charge order in the kagome metal AV3sb5 (  $a=k,rb,cs$  ), *Phys. Rev. Lett.* **127**, 217601 (2021).
- [22] Y.-P. Lin and R. M. Nandkishore, Complex charge density waves at van hove singularity on hexagonal lattices: Haldane-model phase diagram and potential realization in the kagome metals AV3sb5 (  $a=k,rb,cs$  ), *Phys. Rev. B* **104**, 045122 (2021).
- [23] W. Ruan, X. Li, C. Hu, Z. Hao, H. Li, P. Cai, X. Zhou, D.-H. Lee, and Y. Wang, Visualization of the periodic modulation of cooper pairing in a cuprate superconductor, *Nat. Phys.* **14**, 1178 (2018).
- [24] H.-S. Xu, Y.-J. Yan, R. Yin, W. Xia, S. Fang, Z. Chen, Y. Li, W. Yang, Y. Guo, and D.-L. Feng, Multiband superconductivity with sign-preserving order parameter in kagome superconductor CsV3sb5, *Phys. Rev. Lett.* **127**, 187004 (2021).
- [25] S. Ni, S. Ma, Y. Zhang, J. Yuan, H. Yang, Z. Lu, N. Wang, J. Sun, Z. Zhao, D. Li, S. Liu, H. Zhang, H. Chen, K. Jin, J. Cheng, L. Yu, F. Zhou, X. Dong, J. Hu, H.-J. Gao, and Z. Zhao, Anisotropic superconducting properties of kagome metal CsV3sb5, *Chinese Phys. Lett.* **38**, 057403 (2021).
- [26] F. H. Yu, D. H. Ma, W. Z. Zhuo, S. Q. Liu, X. K. Wen, B. Lei, J. J. Ying, and X. H. Chen, Unusual competition of superconductivity and charge-density-wave state in a compressed topological kagome metal, *Nat. Commun.* **12**, 23928 (2021).
- [27] F. Du, S. Luo, B. R. Ortiz, Y. Chen, W. Duan, D. Zhang, X. Lu, S. D. Wilson, Y. Song, and H. Yuan, Pressure-induced double superconducting domes and charge instability in the kagome metal KV3sb5, *Phys. Rev. B* **103**, 1220504 (2021).
- [28] L. Yin, D. Zhang, C. Chen, G. Ye, F. Yu, B. R. Ortiz, S. Luo, W. Duan, H. Su, J. Ying, S. D. Wilson, X. Chen, H. Yuan, Y. Song, and X. Lu, Strain-sensitive superconductivity in the kagome metals KV3sb5 and CsV3sb5 probed by point-contact spectroscopy, *Phys. Rev. B* **104**, 174507 (2021).
- [29] T. Wang, A. Yu, H. Zhang, Y. Liu, W. Li, W. Peng, Z. Di, D. Jiang, and G. Mu, Enhancement of the superconductivity and quantum metallic state in the thin film of superconducting kagome metal kv3sb5, (2021), [arXiv:2105.07732 \[cond-mat.supr-con\]](#).
- [30] B. Q. Song, X. M. Kong, W. Xia, Q. W. Yin, C. P. Tu, C. C. Zhao, D. Z. Dai, K. Meng, Z. C. Tao, Z. J. Tu, C. S. Gong, H. C. Lei, Y. F. Guo, X. F. Yang, and S. Y. Li, Competing superconductivity and charge-density wave in kagome metal csv3sb5: evidence from their evolutions with sample thickness, (2021), [arXiv:2105.09248 \[cond-mat.supr-con\]](#).
- [31] Y. Song, T. Ying, X. Chen, X. Han, X. Wu, A. P. Schnyder, Y. Huang, J. gang Guo, and X. Chen, Competition of superconductivity and charge density wave in selective oxidized CsV3sb5 thin flakes, *Phys. Rev. Lett.* **127**, 237001 (2021).
- [32] H. Tan, Y. Liu, Z. Wang, and B. Yan, Charge density waves and electronic properties of superconducting kagome metals, *Phys. Rev. Lett.* **127**, 046401 (2021).
- [33] L. Fu and C. L. Kane, Topological insulators with inversion symmetry, *Physical Review B* **76**, 045302 (2007).
- [34] B. R. Ortiz, S. M. Teicher, L. Kautzsch, P. M. Sarte, N. Ratcliff, J. Harter, J. P. Ruff, R. Seshadri, and S. D. Wilson, Fermi surface mapping and the nature of charge-density-wave order in the kagome superconductor CsV3sb5, *Physical Review X* **11**, 041030 (2021).
- [35] L. Fu and E. Berg, Odd-parity topological superconductors: Theory and application to  $Cu_xBi_2Se_3$ , *Physical Review Letters* **105**, 097001 (2010).
- [36] Z. Wang, P. Zhang, G. Xu, L. K. Zeng, H. Miao, X. Xu, T. Qian, H. Weng, P. Richard, A. V. Fedorov, H. Ding, X. Dai, and Z. Fang, Topological nature of the FeSe0.5Te0.5 superconductor, *Physical Review B* **92**, 115119 (2015).
- [37] T. Sato, Y. Tanaka, K. Nakayama, S. Souma, T. Takahashi, S. Sasaki, Z. Ren, A. A. Taskin, K. Segawa, and Y. Ando, Fermiology of the strongly spin-orbit coupled superconductor  $Sn_{1-x}In_xTe$ : Implications for topological superconductivity, *Physical Review Letters* **110**, 206804 (2013).
- [38] J.-Y. You, B. Gu, G. Su, and Y. P. Feng, Two-dimensional topological superconductivity candidate in a van der waals layered material, *Physical Review B* **103**, 104503 (2021).
- [39] S. Peng, Y. Han, G. Pokharel, J. Shen, Z. Li, M. Hashimoto, D. Lu, B. R. Ortiz, Y. Luo, H. Li,

- M. Guo, B. Wang, S. Cui, Z. Sun, Z. Qiao, S. Wilson, and J. He, Realizing kagome band structure in two-dimensional kagome surface states of  $\text{RV}_6\text{Sn}_6$  (  $r=\text{gd}$  ,  $\text{ho}$ ), *Phys. Rev. Lett.* **127**, 266401 (2021).
- [40] G. Pokharel, S. M. L. Teicher, B. R. Ortiz, P. M. Sarte, G. Wu, S. Peng, J. He, R. Seshadri, and S. D. Wilson, Electronic properties of the topological kagome metals  $\text{YV}_6\text{Sn}_6$  and  $\text{GdV}_6\text{Sn}_6$ , *Phys. Rev. B* **104**, 235139 (2021).